

Carbon-nitrogen coupling and algal-bacterial interactions during an experimental bloom: Modeling a ^{13}C tracer experiment

*Karel Van den Meersche*¹

Netherlands Institute of Ecology, Korrिंगaweg 7, 4401 NT Yerseke, The Netherlands; University of Gent, Biology Department, Marine Biology Section, Krijgslaan 281, S8, 9000 Gent, Belgium

Jack J. Middelburg, Karline Soetaert, Pieter van Rijswijk, and Henricus T. S. Boschker

Netherlands Institute of Ecology, Korrिंगaweg 7, 4401 NT Yerseke, The Netherlands

Carlo H. R. Heip

Netherlands Institute of Ecology, Korrिंगaweg 7, 4401 NT Yerseke, The Netherlands; University of Gent, Biology Department, Marine Biology Section, Krijgslaan 281, S8, 9000 Gent, Belgium

Abstract

We tracked flows of carbon and nitrogen during an experimental phytoplankton bloom in a natural estuarine assemblage in Randers Fjord, Denmark. We used ^{13}C -labeled dissolved inorganic carbon to trace the transfer of carbon from phytoplankton to bacteria. Ecosystem development was followed over a period of 9 d through changes in the stocks of inorganic nutrients, pigments, particulate organic carbon and nitrogen, dissolved organic carbon (DOC), and algal and bacterial polar-lipid-derived fatty acids (PLFA). We quantified the incorporation of ^{13}C in phytoplankton and bacterial biomass by carbon isotope analysis of specific PLFA. A dynamic model based on unbalanced algal growth and balanced growth of bacteria and zooplankton adequately reproduced the observations and provided an integral view of carbon and nitrogen dynamics. There were three phases with distinct carbon and nitrogen dynamics. During the first period, nutrients were replete, an algal bloom was observed, and carbon and nitrogen uptake occurred at a constant ratio. Because there was little algal exudation of DOC, transfer of ^{13}C from phytoplankton to bacteria was delayed by 1 d, compared with the labeling of phytoplankton. In the second phase, the exhaustion of dissolved inorganic nitrogen resulted in decoupling of carbon and nitrogen flows caused by unbalanced algal growth and the exudation of carbon-rich dissolved organic matter by phytoplankton. During the final, nutrient-depleted phase, carbon and nitrogen cycling were dominated by the microbial loop and there was accumulation of DOC. The main source (60%) of DOC was exudation by phytoplankton growing under nitrogen limitation. Heterotrophic processes were the main source of dissolved organic nitrogen (94%). Most of the carbon exudated by algae was respired by the bacteria and did not pass to higher trophic levels. The dynamic model successfully reproduced the evolution of trophic pathways during the transition from nutrient-replete to -depleted conditions, which indicates that simple models provide a powerful tool to study the response of pelagic ecosystems to external forcings.

Understanding the transfer of carbon and nutrients between the environment and autotrophs and heterotrophs is key to furthering our knowledge on biogeochemical cycling and ecosystem functioning and how both relate. Ecologists have long distinguished two trophic pathways in the pelagic environment—the herbivorous or classical food web and the microbial loop—but now acknowledge the existence of a continuum of trophic structures with the herbivorous food

web and the microbial loop as end members (Legendre and Rassoulzadegan 1995). The different trophic pathways within this continuum may shift seasonally or after a disturbance, with the result that nutrient use changes at the community level. Similarly, the traditional biogeochemical paradigm that the use and release of nutrients at the ecosystem level obeys a simple constant stoichiometry (the Redfield ratio), recorded in the fixed ratio of C to N and P in seston (Redfield et al., 1963), has been successfully challenged. Temporal decoupling of carbon and nutrient dynamics has been reported repeatedly after bloom events (Engel et al. 2002; Wetz and Wheeler 2003) and is reflected, for instance, in the temporal accumulation of carbon-rich dissolved organic matter (DOM; Duursma 1961; Sondergaard et al. 2000), increases in the particulate C:N ratio, and the formation of transparent carbon-rich exopolymeric particles (Alldredge et al. 1995). The decoupling of carbon and nutrient cycling at the community level is related to the different abilities of autotrophs and heterotrophs to maintain homeostasis (Sterner and Elser 2003) and to the different dynamics of the particulate and DOM pools (Banse 1994).

¹ Corresponding author (K.vdMeersche@nioo.knaw.nl).

Acknowledgments

We thank Joop Nieuwenhuize for analytical and logistic support, our Eurotroph colleagues for a stimulating research environment, and two anonymous reviewers for constructive feedback. We thank Wim Vyverman and Luc De Meester for constructive remarks. The modeling part of this research was performed in the frame of a master's thesis at Ghent University (K.V.d.M.).

The present research was supported by the European Union (Eurotroph, EVK3-CT-2000-00040) and a PIONEER grant from the Netherlands Organization of Scientific Research (833.02.2002).

This is contribution 3260 from the Netherlands Institute of Ecology.

In all organisms, the carbon and nitrogen cycles are closely linked (Sterner and Elser 2003), but the coupling between carbon and nitrogen economy in heterotrophs (bacteria and higher trophic levels) and algae differs in many respects. First, bacteria have a higher basic nitrogen requirement for proteins and nucleic acids and, therefore, a lower C:N ratio than most algae. Heterotrophs also maintain relatively narrow stoichiometric ranges for C and N in their biomass. This is in contrast to resource investments in algae that are not as closely coupled but are regulated by their physiological condition. To secure growth, their carbon and nitrogen acquisition must be coordinated but not necessarily coupled in time, and the C:N ratio of algae can be quite variable. Algae use the carbon acquired by photosynthesis during the day for nitrogen assimilation and biosynthesis during the night until the exhaustion of photosynthesis products. In contrast to phytoplankton, heterotrophs are not directly dependent on light intensity, but they need the products produced by the algae for growth. Higher trophic levels derive their energy from algal tissue either directly (grazers) or indirectly (predators). The direct link from algae to bacteria is via DOM, the main source of bacterial carbon and the preferred source of bacterial nitrogen (Wheeler and Kirchman 1986; Kirchman 1994). Algae produce DOM through lysis, passive leakage, or exudation of carbon-rich material (Anderson and Williams 1998), but there are other sources of DOM as well that are either indirectly linked to or independent of algal dynamics. These include enzymatic hydrolysis of particulate material through bacteria (Smith et al. 1992), sloppy feeding and incomplete digestion by grazers (Jumars et al. 1989), and bacterial mortality after viral lysis (Cotner and Biddanda 2002). Conversely, algae depend on the ammonium regenerated by bacteria and higher trophic levels for their growth. All of this indicates that the carbon and nitrogen metabolism of algae and heterotrophs are related but not necessarily synchronized. For instance, there is ample evidence that bacteria respond to increased primary production with a variable time lag of a couple of days (Ducklow et al. 1993).

Our ability to test or quantify the couplings of algae and heterotrophs in nature or between nitrogen and carbon cycles depends on acquiring a good data set. Such data should be of sufficient temporal resolution and include the necessary measurements that can constrain the many unknown fluxes. Simple standing stock measurements may give an indication of how the system works but are generally not sufficient to make quantitative statements with reasonable accuracy (Valiño 2000). This is because biomass changes are the net result of many processes that operate at the same time. The deliberate introduction of a tracer such as ^{13}C -labeled dissolved inorganic carbon (DIC) under controlled conditions, and its consequent tracking into the various components, provides valuable extra constraints (Norrman et al. 1995; Lyche et al. 1996; Cole et al. 2002). It allows one to pinpoint which pathways are significant and to identify the main players of the ecosystem. Through analysis of the concentration of specific biomarkers for algae and bacteria and the appearance of labels in these substances (Boschker and Middelburg 2002), it is now possible to resolve algal-bacterial interactions using stable isotopes (Middelburg et al. 2000).

In combination with mathematical modeling, such data

may also serve to estimate the fluxes and turnover rates. To date, a number of physiologically based models exist that describe the uncoupling of C and N assimilation in algae (so-called unbalanced growth models), through the build up and consumption of either energy storage reserves (Lancelot and Billen 1985) or an intracellular nitrogen pool (Droop 1973; Tett 1998). These formulations have proved their worth in simulations of culture (Geider et al. 1998) and seasonal (Lancelot et al. 1991; Soetaert et al. 2001; Flynn and Fasham 2003) data. Similarly, a suite of models exists that explicitly deal with C and N acquisition in bacteria (Anderson and Williams 1998). Although these formulations provide an idealized outline as to how algal and bacterial organisms function, we still need to progress in our understanding and prediction capacity of how both work together in an ecosystem context.

For the present article, we used a combined experimental modeling approach to investigate C and N dynamics within the microbial domain during an exponential bloom. We specifically tried to assess the coupling between algae and bacteria and between carbon and nitrogen during and after the bloom. To do so, we added ^{13}C -labeled DIC and followed the fate of ^{13}C for 9 d within an enclosure. The biomass and incorporation of label into bacteria and algae was tracked through specific polar-lipid-derived fatty acids (PLFA). A coupled carbon-nitrogen- ^{13}C model was then used to quantify the carbon and nitrogen fluxes between the different compartment and organisms during the transition from nutrient-replete to -depleted conditions.

Materials and Methods

Experiment—The experiment took place in Randers Fjord Estuary, Denmark ($56^{\circ}35'\text{N}$, $10^{\circ}22'\text{E}$) during 21–30 August 2001. Water was collected from the freshwater end of the Randers Fjord. The salinity of the water was 0.2, and riverine dissolved inorganic nutrient and DIC concentrations were high (58 mmol N m^{-3} , $1.1 \text{ mmol P m}^{-3}$, $226 \text{ mmol Si m}^{-3}$, and 2.1 mol C m^{-3}), although they were comparable to those in coastal upwelling systems, except for the high dissolved inorganic N:P ratio and Si concentrations. At 1200 h on 21 August 2001, two 80-liter, transparent carboys were filled with 60 liters of ambient water, and 10 ml of $0.5 \text{ mol L}^{-1} \text{ }^{13}\text{C}\text{-DIC}$ ($>98\% \text{ }^{13}\text{C}$) was added to a final concentration of $8.3 \text{ } \mu\text{mol L}^{-1}$ ($<3\%$ of total stock). After closing the containers, they were left floating in the water. For a period of 9 d, the water was sampled eight times (after 0, 4, 24, 48, 72, 120, 168, and 204 h), and the temperature and pH were measured. The carboys were vigorously mixed manually before sampling $\sim 4\text{--}6$ liters. Approximately 750 ml of water was filtered through preweighted, precombusted Whatman GF/F filters, which were stored at -20°C and later analyzed for particulate nitrogen (PN) and organic carbon (POC) using an elemental analyzer (Nieuwenhuize et al. 1994). The carbon isotopic composition of the particulate material was measured using a Carlo Erba Elemental analyzer coupled on line to a Finnigan Delta S isotope ratio mass spectrometer (IRMS). GF/F-filtered water was stored frozen or at 4°C and was later analyzed for various com-

pounds. Concentrations of silicate, phosphate, ammonium, nitrate, and nitrite were measured by automated colorimetric techniques (Middelburg and Nieuwenhuize 2000). For analysis of photosynthetic pigments, another portion of water (500–750 ml) was filtered through GF/F filters that were stored frozen until analysis by high-performance liquid chromatography (Barranguet et al. 1997). Samples for DIC and $\delta^{13}\text{C}$ -DIC were collected in headspace vials (50 ml) and preserved with mercury chloride. In the laboratory, an He headspace was created, and the concentration and isotopic composition of carbon dioxide in the headspace were measured using an elemental analyzer coupled to a Finnigan Delta XL IRMS (Moodley et al. 2000). Samples for DOC (20 ml) were filtered through precombusted GF/F filters, stored frozen, and analyzed using a combined ultraviolet–wet oxidation technique. Approximately 2 liters of water was filtered through GF/F filters for subsequent measurement of PLFA concentration and isotopic composition. In brief, algal and bacterial PLFA were extracted according to the method of Boschker et al. (1999) and Middelburg et al. (2000) and were measured using gas chromatography (GC) with flame ionization detection. The incorporation of ^{13}C in phytoplankton and bacterial biomass was quantified by carbon isotope analysis of specific PLFA using GC-combustion IRMS (Boschker and Middelburg 2002).

Phytoplankton and bacterial carbon concentrations were calculated from the PLFA concentrations as described in Middelburg et al. (2000). From the specific bacterial PLFA, total bacterial C concentration can be calculated as

$$C_{\text{bact}} = \sum \frac{\text{PLFA}_{\text{bact}}}{a} = \sum \frac{\text{PLFA}_{\text{bact,spec}}}{(a \times b)}$$

where a is the average PLFA concentration in bacteria (0.073 g of carbon PLFA per gram of carbon biomass for aerobic environments, Brinch-Iversen and King 1990) and $b = 0.14$ g specific bacterial PLFA (i14:0, i15:0, and a15:0) per gram of bacterial PLFA content (Moodley et al. 2000). Phytoplankton concentration was calculated from the difference between total PLFA and bacterial PLFA as

$$C_{\text{phyto}} = \frac{\sum \text{PLFA} - \sum \text{PLFA}_{\text{bact}}}{c}$$

The average concentration of PLFA in algae ($c = 0.046$ g PLFA-carbon g carbon biomass $^{-1}$) was estimated by linear regression between $(\text{POC} - C_{\text{bact}})$ and $\text{PLFA}_{\text{phyto}}$, under the assumption that detritus concentrations were negligible at the start of the experiment. This value is significantly higher than that reported by Middelburg et al. (2000), $c = 0.035$, but including an initial detritus concentration would only increase the estimated value (see below). These conversion factors (a , b , and c) introduce significant uncertainty ($\sim 50\%$) to biomass estimates, but they do not affect the temporal evolution of biomass patterns or the transfer dynamics of ^{13}C from algae to bacteria.

Model—The data set obtained from the enclosure experiments was analyzed with a mathematical model, to test the internal consistency of the various measurements and to quantify the fluxes between the compartments. Because of

the limited size of the carboys, a vertical gradient was neglected, and a zero-dimensional model was implemented. The model was driven by photosynthetically active irradiance, which was imposed as a forcing function (Fig. 1). Hourly data were available from the Danish Institute for Agricultural Sciences from a nearby site. In addition, the temperature and pH, as measured daily in the experiment vessels, were imposed on the model (Fig. 1). The model was implemented on a personal computer in the model environment FEMME (Soetaert et al. 2002), and the code is available on request from the authors. All model equations are shown in table 3, model parameters are in table 1, and model variables are in table 2. Equations were based on the model of Anderson and Williams (1998; hereafter referred to as A&W) but with spatial components eliminated and including a number of essential modifications related to unbalanced algal growth. The model of A&W describes fluxes in terms of nitrogen among three living (bacterial N, phytoplankton N, and zooplankton N), one detrital, and four DOM pools (labile and semilabile dissolved organic carbon [DOC] and dissolved organic nitrogen [DON]) and two nutrients (nitrate and ammonium). Total carbon fluxes and ^{13}C carbon fluxes accompanying the nitrogen fluxes were first added to this model. Because all biological and chemical processes are temperature dependent, a temperature limitation factor was included in every equation term (Eq. 1).

The data showed significant variations in the C:N ratio of total particulate organic matter, which could not be reproduced with the original A&W model, in which all particulate constituents have a constant C:N ratio. Therefore, a variable C:N ratio in phytoplankton and detritus had to be considered. The variation of the C:N ratio in phytoplankton was based on the unbalanced growth model of Tett (1998), as implemented in the model of Soetaert et al. (2001). In this model, the N and C uptake (Eqs. 4, 7) are uncoupled through the luxury uptake of dissolved inorganic nitrogen. Also, the detritus breakdown rates were made dependent on the detritus C:N ratio under the assumption that nitrogen-depleted fractions are more refractory and nitrogen-rich fractions are more labile (Smith and Tett 2000; Soetaert et al. 2001) (eqs. 38–42). A significant decrease in DIC concentration (down to 780 mol C m^{-3}) justified the need to introduce a carbon limitation factor in the phytoplankton carbon uptake rate (Eq. 9). Chlorophyll a concentrations were modeled as described in Soetaert et al. (2001), depending on the phytoplankton concentration and the phytoplankton C:N ratio (eqs. 53–54).

In the A&W model, DOC is actively released by phytoplankton, to compensate for the luxury carbon uptake caused by shifts in environmental factors such as light availability and nutrient depletion (Mague et al. 1980; Williams 1990). Two formulations are presented in A&W: active DOC release as a constant fraction of the primary production, and thus depending on light, or release, depending on the nutrient stressed condition of the algae (related to both light and nutrient availability). We implemented the second option (eq. 10), because the model showed an improved accordance between predicted and observed values when this formulation was used. Unlike A&W, however, carbon uptake in our model is not dependent on nutrient limitation (a function of ex-

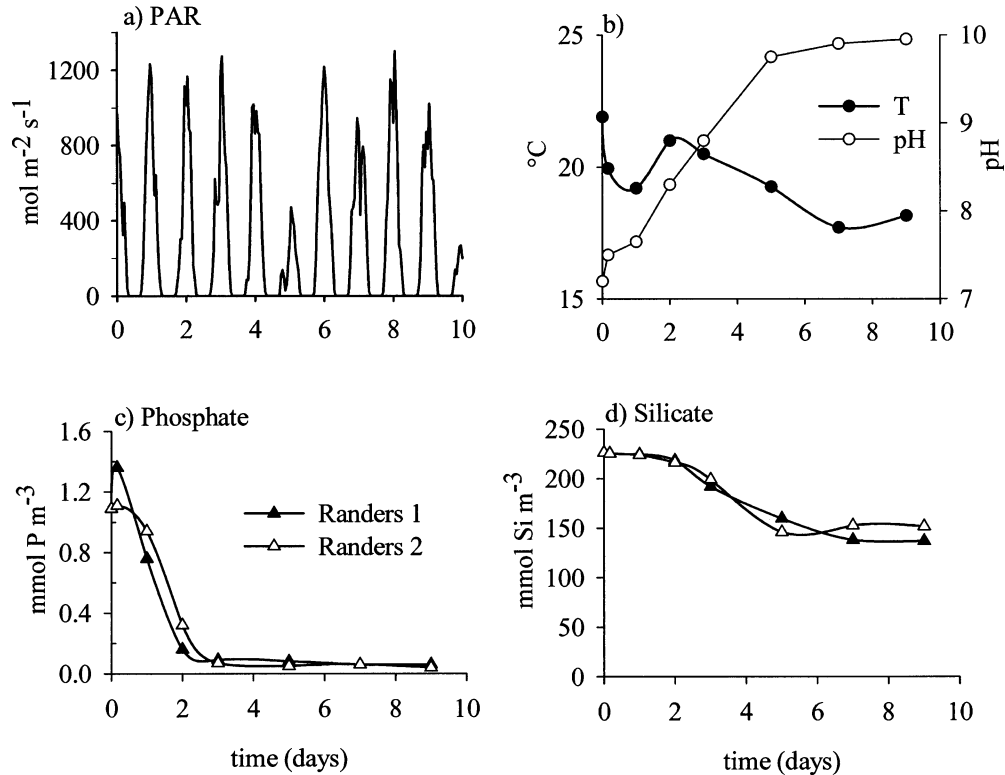


Fig. 1. Temporal evolution of forcing parameters, dissolved inorganic phosphate, and silicate. The two replicate experiments (Randers 1 and 2) are presented with different symbols. (a) Photosynthetically active radiation data were measured in air using a LICOR sensor LI-190SA (400–700 nm; data from Foulum, ~25 km from the center of the city of Randers, courtesy of the Danish Institute of Agricultural Sciences), (b) temperature and pH, (c) dissolved inorganic phosphate, and (d) dissolved silicate.

ternal nutrient concentration) but on the internal C:N ratio in phytoplankton (eq. 7). Extra carbon overflow is calculated as a fraction of the difference between the nutrient-limited (actual C:N ratio) and nutrient-saturated (minimum C:N ratio) growth rate. This explains the limitation factor in equation 10:

$$\frac{\theta_p - \min \theta_p}{\max \theta_p} = \left(1 - \frac{\min \theta_p}{\max \theta_p}\right) - \left(1 - \frac{\theta_p}{\max \theta_p}\right)$$

which is the difference between the physiological limitation factors for minimum and actual C:N ratio, respectively.

Zooplankton grazing and mortality were modeled as in A&W (eqs. 19, 25), and excretion and respiration terms were added in the nitrogen and carbon uptake equations, respectively (eq. 16). Constant zooplankton stoichiometry (homeostasis) is regulated through excretion and respiration; if the nitrogen content of the ingested food is too high, excess nitrogen is excreted (eq. 23). If the food contains too little nitrogen, the carbon surplus will be respired (eq. 24). The bacterial and DOC-DON dynamics are kept as in A&W (eqs. 26–35), except for the bacterial mortality rate, which is assumed to be proportional to the bacterial concentration (second-order mortality), because viral infection causing cell lysis increases with the concentration (Cotner and Biddanda 2002) (eq. 36).

The experiments took place in a very small, enclosed en-

vironment, and DIC concentrations and the pH varied considerably (Figs. 1, 3). As a result, $p\text{CO}_2$ changed from highly supersaturated at the start to undersaturated at the end of the experiment. CO_2 exchange with the atmosphere was therefore considered, as similarly described in Cole et al. (2002) (eq. 52). CO_2 partial pressure was calculated in the model using the pH, temperature (both forcing functions), DIC concentration (a state variable), and thermodynamic solubility of CO_2 at the prevailing temperature and salinity (Millero 1995). The gas piston velocity was obtained from model fitting and had little physical relevance, because the air-sea exchange was taking place in closed containers.

The ^{13}C cycle was described, following the same pathways as the total carbon ($^{13}\text{C} + ^{12}\text{C}$) cycle and using the same process parameters. In short, for each C flux, a corresponding ^{13}C flux was calculated and made proportional with the ^{13}C content of the source compartment

$$F_{x,^{13}\text{C}} = F_{x,\text{C}} \times \frac{X_{^{13}\text{C}}}{X_{\text{C}}}$$

where $F_{x,^{13}\text{C}}$ and $F_{x,\text{C}}$ represent fluxes of ^{13}C and total C respectively, and $X_{^{13}\text{C}}/X_{\text{C}}$ is the fraction of ^{13}C in the flux source compartment.

Results

Experiment—The two enclosure experiments exhibited similar temporal behavior and will therefore be considered

Table 1. Model parameters.

Symbol	Value	Units	Description	Source
α	0.015	$\mu\text{mol m}^{-2} \text{s}^{-1} \text{d}^{-1}$	Initial slope of $P - I$ curve	A&W (recalculated)
$k_{S_{\text{DIC}}}$	250	mmol C m^{-3}	Half-saturation constant for algal C uptake	Fitted
$k_{N_{\text{N}}}$	0.5	mmol N m^{-3}	Half-saturation constant for algal nitrate uptake	A&W
$k_{S_{\text{A}}}$	0.5	mmol N m^{-3}	Half-saturation constant for algal ammonium uptake	A&W
Ψ	1.5	$\text{m}^3 \text{mmol N}^{-1}$	NH_3 inhibition constant for phytoplankton nitrate uptake	A&W
m_p	0.045	d^{-1}	Phytoplankton-specific mortality rate	A&W
γ_l	0.02	—	Phytoplankton leakage fraction	Fitted
$\Gamma_{P,A}$	0.1	—	Phytoplankton activity respiration fraction	Assumed
$r_{P,B}$	0.01	d^{-1}	Phytoplankton basal respiration rate	Assumed
E	0.34	—	Phytoplankton mortality losses to DOM	A&W
γ_3	0.05	—	Ratio of extra DOC produced by N limitation	Fitted
μ_p	5.5	d^{-1}	Phytoplankton maximum C uptake rate	Fitted
$\mu_{P,A}$	2	$\text{mol N mol C}^{-1} \text{d}^{-1}$	Phytoplankton maximum ammonium uptake rate	Fitted
$\mu_{P,Nn}$	2	$\text{mol N mol C}^{-1} \text{d}^{-1}$	Phytoplankton maximum nitrate uptake rate	Fitted
max θ_p	20	mol C mol N^{-1}	Maximum phytoplankton C:N ratio	Soetaert et al. (2001)
min θ_p	6	mol C mol N^{-1}	Minimum phytoplankton C:N ratio	Soetaert et al. (2001)
max η_p	2	g Chl mol N^{-1}	Maximum Chl a :N ratio in phytoplankton	Soetaert et al. (2001)
min η_p	1.4	g Chl mol N^{-1}	Minimum Chl a :N ratio in phytoplankton	Soetaert et al. (2001)
θ_z	6.625	mol C mol N^{-1}	Zooplankton C:N ratio	Assumed (Redfield)
g	1.0	d^{-1}	Zooplankton maximal grazing rate	A&W
B	0.75	—	Zooplankton assimilation efficiency	A&W
p_1	0.333	—	Zooplankton preference for phytoplankton food	A&W
p_2	0.333	—	Zooplankton preference for bacterial food	A&W
p_3	0.333	—	Zooplankton preference for detrital food	A&W
k_g	1.0	mmol N m^{-3}	Half-saturation food concentration for zooplankton grazing	A&W
Φ	0.23	—	Feeding losses to DOM	A&W
$f_{Z,B}$	0.03	d^{-1}	Zooplankton basal respiration rate	Assumed
$f_{Z,A}$	0.25	—	Fraction of zooplankton C uptake that is respired	Assumed
m_z	0.3	d^{-1}	Zooplankton specific mortality rate	A&W
K_{mz}	0.2	mmol N m^{-3}	Zooplankton half-saturation for mortality	A&W
μ_B	13.3	d^{-1}	Maximum bacterial labile DOC uptake	A&W
μ_S	4	d^{-1}	Maximum bacterial semilabile DOC hydrolysis rate	A&W
Ω	0.19	mol C mol C^{-1}	Bacterial gross growth efficiency	Fitted
θ_B	5.1	mol C mol N^{-1}	Bacterial C:N ratio	A&W
k_L	25	mmol C m^{-3}	Half-saturation value for bacterial labile DOC uptake	A&W
k_A	0.5	mmol N m^{-3}	Half-saturation value for bacterial ammonium uptake	A&W
k_S	417	mmol C m^{-3}	Half-saturation value for bacterial semilabile DOC hydrolysis	A&W
m_B	0.05	d^{-1}	Bacteria specific mortality rate	Fitted
$\theta_{D,\text{max}}$	15	mol C mol N^{-1}	Maximal C:N ratio of detritus	Assumed
$R_{C,\text{max}}$	0.29	d^{-1}	Maximal degradation rate of detrital C at 20°C	Assumed
$R_{N,\text{max}}$	0.33	d^{-1}	Maximal degradation rate of detrital N at 20°C	Assumed
Y	0.03	d^{-1}	Nitrification rate	A&W
Δ	0.65	—	Part of grazing and mortality DOM flux to labile DOM	Fitted
Q_{10}	2.0	—	Q_{10} for temperature dependent rates	Soetaert et al. (2001)
Salinity	0.2	—	—	Measured
K	0.06	$\text{mmol C m}^{-3} \mu\text{atm}^{-1} \text{d}^{-1}$	Gas exchange coefficient	Fitted
PCO_2atm	360	μatm	Partial pressure of CO_2 in the atmosphere	—
KC1	4.3×10^{-7}	—	Dissociation constant of H_2CO_3 at 0 salinity and 20°C	—
KC2	5.61×10^{-11}	—	Dissociation constant of HCO_3^- at 0 salinity and 20°C	—
K0	3.7×10^{-2}	$\text{mmol C m}^{-3} \mu\text{atm}^{-1}$	Solubility of CO_2 in water (Henry's law), 0.2 salinity, and 20°C	Millero (1995)

to be replicates (Figs. 1 to 3). The experiment started off with low values of particulate organic matter (both living and nonliving), with a high C:N ratio (10 mol C mol N⁻¹) and high dissolved inorganic nutrient concentrations (ammonium 1.9 mmol N m⁻³, nitrate 56.1 mmol N m⁻³, phosphate 1.1 mmol P m⁻³, and silicate 226 mmol Si m⁻³). These conditions triggered the onset of an algal bloom that ended at 1200 h on day 4. During this period, chlorophyll concentrations increased exponentially, almost two orders of mag-

nitude (3.6–100 mg Chl a m⁻³; Fig. 2f). After the exhaustion of inorganic nitrogen and phosphate (Figs. 1c, 3c,d), the bloom ended. Ammonium (Fig. 3d) was consumed first, followed a few days later by nitrate (Fig. 3c). Dissolved Si remained well above limiting concentrations (Fig. 1d). The decrease in the C:N ratio observed in particulate organic matter at this stage (10–7 mol C mol N⁻¹) reflected the growth of fresh algal biomass (with a low C:N ratio) that diluted the refractory detrital matter present (Fig. 2c).

The postbloom phase was characterized by low nutrient conditions with concentrations of ~ 1 mmol $\text{NO}_3^- \text{m}^{-3}$ and ~ 0.2 mmol $\text{NH}_4^+ \text{m}^{-3}$. During this phase, chlorophyll concentrations decreased significantly, from 100 mg m^{-3} on day 4 to 50 mg m^{-3} on day 9. The phytoplankton carbon content based on PLFA concentrations also decreased but at a lower rate (Fig. 2e). The nutrient exhaustion also induced large changes in the physiological status of the algae: the C:N ratio of particulate organic matter more than doubled, up to $16 \text{ mol C mol N}^{-1}$, which indicates a decoupling of carbon and nitrogen dynamics in phytoplankton. After that, the C:N ratio remained more stable. DOC concentrations were quasi constant at first but increased from 370 to $440 \text{ mmol C m}^{-3}$ after the bloom (Fig. 3b). The bacterial biomass, derived from PLFA concentrations (Fig. 2d), corresponded to DOC concentrations.

Pigment analysis indicated that there was a slight dominance by green algal pigments (chlorophyll *b*, luteine, neoxanthine, and violaxanthine) at the start and an increasing preponderance of diatom pigments (chlorophyll *c*, diadinoxanthine, diatoxanthine, and fucoxanthine) toward the end (Fig. 4). The ratio of diatom to chlorophyta pigments changed from 1.1 during the exponential phase to 3.0 after the bloom, and this dominance of diatoms was consistent with silicate concentrations, which remained well above limiting values (Fig. 1d). The concentration of cyanobacterial pigments (zeaxanthine) remained low, although they kept increasing until the end of the experiment. Concentrations of algal-specific PLFA showed the same trend as algal pigments, which supports the dominance of diatoms and green algae in the enclosures (data not shown).

Carbon-13 was added as a deliberate tracer to follow carbon transfer from the DIC pool to algae and then to bacteria. After adding ^{13}C -DIC, the $\delta^{13}\text{C}$ of DIC increased to $2,675\text{‰}$, which is equivalent to a $^{13}\text{C}/\text{C}$ fraction of 2.5%. $\delta^{13}\text{C}$ -DIC decreased to $\sim 2,200\text{‰}$ toward the end of the experiment. Particulate organic $\delta^{13}\text{C}$ increased from background values of -29‰ to $\sim 2,200\text{‰}$ in ~ 4 d, because of dilution with newly fixed ^{13}C -rich carbon, and then stabilized. This ^{13}C enrichment was more dramatic for phytoplankton $\delta^{13}\text{C}$ values, which increased to $> 2,200\text{‰}$ within 3 d. Bacterial $\delta^{13}\text{C}$ increased with a delay of ~ 1 d and attained $\sim 2,200\text{‰}$ after 6 d. For comparison with the model, ^{13}C fractions [$^{13}\text{C}/(^{13}\text{C} + ^{12}\text{C})$] are presented rather than $\delta^{13}\text{C}$, because they are easier to interpret (Fig. 5). The bulk POC, phytoplankton, and bacterial pools all reached the same asymptotic enrichment level of 2.5%, which indicates that these pools were in isotopic equilibrium on day 5. In summary, three phases could be distinguished in the experiment (Figs. 2, 3): (1) an exponential growth or bloom phase (days 1–3) with sufficient nutrients, (2) an unbalanced growth or intermediate phase (days 4–7) with nutrient depletion and ongoing algal production, and (3) a postbloom or stationary phase (days 8–9) with DOC and bacterial biomass accumulation.

Model initialization—Our dynamic model required the specification of 23 initial conditions. Some of them (ammonium, nitrate, and DIC) were measured directly, but many needed to be estimated. At the start of the experiment, a high POC:PN ratio ($10.2 \text{ mol C mol N}^{-1}$) was found. This ratio

reflects the C:N ratio of algae and detritus, the two dominant pools contributing to the particulate organic matter pool. Because high C:N ratios of algae are not expected in a nutrient-rich environment, we imposed an initial value of C:N = 6 for phytoplankton and were able to derive an initial refractory detritus fraction with high C:N ratio ($20 \text{ mol C mol N}^{-1}$). This refractory material could originate from the common reed fields in the surroundings of the sampling location or other upstream sources. Initial algal carbon and nitrogen contents were estimated from measured chlorophyll using eqs. 53 and 54 (Table 3). No macrozooplankton was observed in the experiments, and microzooplankton predation was not determined. The decrease of chlorophyll during the second half of the experiments (days 5–9), which was accompanied by small phytoplankton carbon and POC decreases, could only be reproduced under the assumption of a small initial zooplankton concentration, which in the end caused a reduction of phytoplankton as a result of grazing. In the model, DOM was divided into three pools: refractory, semilabile, and labile, where the first behaves conservatively. The initial DOC concentration was determined, but the relative amounts of these three pools could not be measured and were obtained by tuning the model. The size of these three pools affects the bacterial uptake rate of carbon and ^{13}C . Fitting demanded an initial labile DOC fraction of 0.8% (8% of semilabile DOC), which is within the range of values found in literature (0–6% in marine systems; Carlson 2002). The concentrations of DON pools were also not measured and were assumed to be 10% of DOC.

Model tuning—Most model parameters (Table 1) were adopted from either A&W or Soetaert et al. (2001), but some parameters related to algal carbon and nutrient acquisition, algal DOM exudation, and bacterial dynamics required tuning to adequately reproduce the observation. Using the original algal growth model (Tett 1998; Soetaert et al. 2001), the algae would have continued to deplete DIC at the end of the experiment, whereas a stabilization of DIC was observed instead (Fig. 3). Therefore, we introduced growth limitation through DIC with a half-saturation constant of $250 \text{ mmol C m}^{-3}$ (eq. 9, table 3), to prevent carbon acquisition in the absence of DIC. Although phytoplankton carbon assimilation was modeled as DIC uptake, we are aware that CO_2 , a small fraction of DIC, is the actual substrate for most algae. This growth reduction could also be related to the high pH values (Fig. 1b), which are detrimental to the integrity of the cell wall. Nitrate and ammonium concentrations decreased abruptly during the phytoplankton bloom phase, and the steepness of this decline was governed by their respective maximum uptake rates. The required maximum uptake rates were found to be higher than the values used in A&W or Soetaert et al. (2001).

Phytoplankton leakage was diminished from 5% in A&W to 2% of the primary production (eqs. 2–3, table 3), to reproduce the limited incorporation of ^{13}C in bacterial biomarkers during the initial bloom phase. Phytoplankton respiration was set at 10% of the primary production, which is well within values observed (5–15%; e.g., Steemann Nielsen and Hansen 1959; Mcallister et al. 1964). The importance of active DOC exudation under nutrient-limited conditions

Table 2. Model variables and forcings.

Variable	Unit	Description
State		
N_P	mmol N m ⁻³	Phytoplankton N concentration
N_Z	mmol N m ⁻³	Zooplankton N concentration
N_B	mmol N m ⁻³	Bacterial N concentration
N_D	mmol N m ⁻³	Detritus N concentration
C_P	mmol C m ⁻³	Phytoplankton C concentration
C_D	mmol C m ⁻³	Detritus C concentration
L_C	mmol C m ⁻³	Dissolved labile organic carbon
S_C	mmol C m ⁻³	Dissolved semilabile organic carbon
DIC	mmol C m ⁻³	Dissolved inorganic carbon (bicarbonate, carbonate, and CO ₂)
L_N	mmol N m ⁻³	Dissolved labile organic nitrogen
S_N	mmol N m ⁻³	Dissolved semilabile organic nitrogen
N_n	mmol N m ⁻³	Nitrate and nitrite concentration
A	mmol N m ⁻³	Ammonium concentration
¹³ C _P	mmol C m ⁻³	Phytoplankton ¹³ C concentration
¹³ C _Z	mmol C m ⁻³	Zooplankton ¹³ C concentration
¹³ C _B	mmol C m ⁻³	Bacterial ¹³ C concentration
¹³ C _D	mmol C m ⁻³	Detritus ¹³ C concentration
¹³ CLabDOC	mmol C m ⁻³	Dissolved labile organic ¹³ C
¹³ C SemiLabDOC	mmol C m ⁻³	Dissolved semilabile organic ¹³ C
¹³ C DIC	mmol C m ⁻³	Dissolved inorganic ¹³ C
Other variables		
F	—	Limitation factor of photosynthesis due to PAR
$Q_C(\text{DIC})$	—	Limitation factor of photosynthesis due to DIC
$Q_{Nn}(N_n, A)$	—	Limitation factor of nitrate uptake due to nitrate and ammonium
$Q_A(A)$	—	Limitation factor of ammonium uptake due to ammonium
$uptN_P$	mmol N m ⁻³ d ⁻¹	Phytoplankton growth
M_P	mmol N m ⁻³ d ⁻¹	Phytoplankton mortality
$R_{P,B}$	mmol C m ⁻³ d ⁻¹	Phytoplankton basal respiration
$R_{P,A}$	mmol C m ⁻³ d ⁻¹	Phytoplankton activity respiration
E	mmol C m ⁻³ d ⁻¹	Extra DOC produced by phytoplankton due to N stress
$uptC_P$	mmol C m ⁻³ d ⁻¹	Phytoplankton carbon uptake rate
$uptN_{n,P}$	mmol N m ⁻³ d ⁻¹	Phytoplankton nitrate uptake rate
$uptA_P$	mmol N m ⁻³ d ⁻¹	Phytoplankton ammonium uptake rate
θ_P	mol C mol N ⁻¹	Phytoplankton C:N ratio
C_Z	mmol C m ⁻³	Zooplankton C concentration
G_P	mmol N m ⁻³ d ⁻¹	Zooplankton grazing rate on phytoplankton
G_B	mmol N m ⁻³ d ⁻¹	Zooplankton grazing rate on bacteria
G_D	mmol N m ⁻³ d ⁻¹	Zooplankton grazing rate on detritus
E_Z	mmol N m ⁻³ d ⁻¹	Zooplankton excretion rate
M_Z	mmol N m ⁻³ d ⁻¹	Zooplankton mortality rate
$AssC_Z$	mmol C m ⁻³ d ⁻¹	Carbon assimilation by zooplankton
$R_{Z,A}$	mmol C m ⁻³ d ⁻¹	Activity respiration of zooplankton
$R_{Z,B}$	mmol C m ⁻³ d ⁻¹	Basal respiration of zooplankton
R_Z	mmol C m ⁻³ d ⁻¹	Respiration of zooplankton
$AssN_Z$	mmol N m ⁻³ d ⁻¹	Nitrogen assimilation by zooplankton
C_B	mmol C m ⁻³	Bacterial C concentration
F_B	mmol N m ⁻³ d ⁻¹	Bacterial growth rate
R_B	mmol C m ⁻³ d ⁻¹	Bacterial respiration
$uptC_B$	mmol C m ⁻³ d ⁻¹	Bacterial uptake of labile DOC
$uptN_B$	mmol N m ⁻³ d ⁻¹	Bacterial uptake of labile DON
$uptA_B^*$	mmol N m ⁻³ d ⁻¹	Potential bacterial uptake of ammonium
$BactDOCHydrolysis$	mmol C m ⁻³ d ⁻¹	Bacterial hydrolysis of semilabile DOC
M_B	mmol N m ⁻³ d ⁻¹	Bacterial mortality
E_B	mmol N m ⁻³ d ⁻¹	Net ammonium excretion of bacteria
ν	mmol N m ⁻³ d ⁻¹	Ammonium oxidation rate
$DissolutionC$	mmol C m ⁻³ d ⁻¹	Dissolution rate of detrital carbon
$DissolutionN$	mmol N m ⁻³ d ⁻¹	Dissolution rate of detrital nitrogen
θ_D	mol C mol N ⁻¹	C:N ratio in detritus
η_P	g Chl mol N ⁻¹	Chlorophyll:N ratio in phytoplankton
Chl a	mg m ⁻³	Chl a concentration, calculated from phytoplankton concentration
CO ₂ flux	mmol C m ⁻³ d ⁻¹	CO ₂ flux from water to air
pCO _{2(water)}	μatm	Partial pressure of CO ₂ in the water

Table 2. Continued.

Variable	Unit	Description
Forcing functions		
I	$\mu\text{mol m}^{-2} \text{s}^{-1}$	Photosynthetically active radiation (PAR, hourly values)
pH	—	Daily measurements
T	$^{\circ}\text{C}$	Temperature (daily measurements)

needed reassessing (γ_3 , eq. 10, table 3), because, in our model with unbalanced algal growth, the phytoplankton C:N ratio (eq. 10) regulates this DOC exudation, instead of direct nutrient limitation, as in A&W. This process highly influences the course of DOM concentrations and C:N ratios, so a value of 0.05 was found to give the best model results, in contrast to 0.26 in A&W. The calculated extra DOC produced varied from 0% to 65% of gross primary production. To prevent DOM accumulation, the labile fraction of produced DOM in the model had to be ~ 0.65 . Preceding modeling studies used fractions varying from 0.1 (A&W) to 0.9 (Levy et al. 1998) to obtain acceptable correspondence (Christian and Anderson 2002).

Bacterial growth efficiency (BGE) and maximal DOC uptake rate govern bacterial ^{13}C signature and carbon concentration. The maximal DOC uptake rate was kept as in A&W, but the BGE had to be altered because lower values gave better fits. According to Del Giorgio and Cole (1998), the BGE for Danish estuaries has a minimal value of 0.19;

this value was therefore adopted. Bacterial mortality only affects bacterial concentration, not the bacterial ^{13}C signature; this process is modeled with a quadratic term (in contrast to A&W), and the bacterial-specific mortality term m_B was obtained by fitting bacterial biomass accumulation.

Model results—Although most model parameters were taken from the literature, it appears that the model captured both the dynamics and size of dissolved and particulate pools (Figs. 2, 3, 5). The model appeared to overpredict POC, PN, and algal concentrations toward the end of the run. This can be attributed to an underestimation of zooplankton grazing, to algal growth on the surfaces, or to sinking of particulate matter to the bottom of the carboys. Those attached or deposited particles are included in the model (because they affect the other components) but not in the measurements, which were based on water samples only. The model was forced by hourly irradiance data and therefore generated daily fluctuations in many variables that either directly (e.g., phytoplankton C) or indirectly (e.g., DOC) depend on primary production. This diurnal variability cannot be discerned in the data because of the daily sampling intervals.

The overall good fit gives us confidence that model-based flux estimates are realistic. Moreover, results from a posteriori comparison of model output for day 1 of the enclosure experiment compared well with independent rate measurement for oxygen dynamics and nitrogen uptake made for the same station during the same week. Model-based rates of net community production and respiration (22 and 6.9 mmol

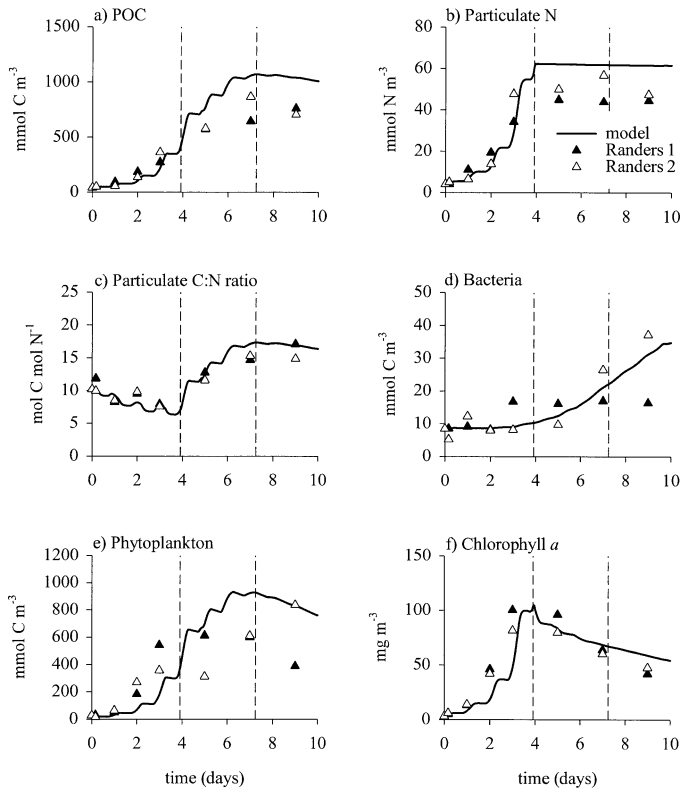


Fig. 2. Temporal evolution of particulate pools for the two enclosure experiments (Randers 1 and 2) and model results (solid line). The three phases are denoted by vertical dashed lines.

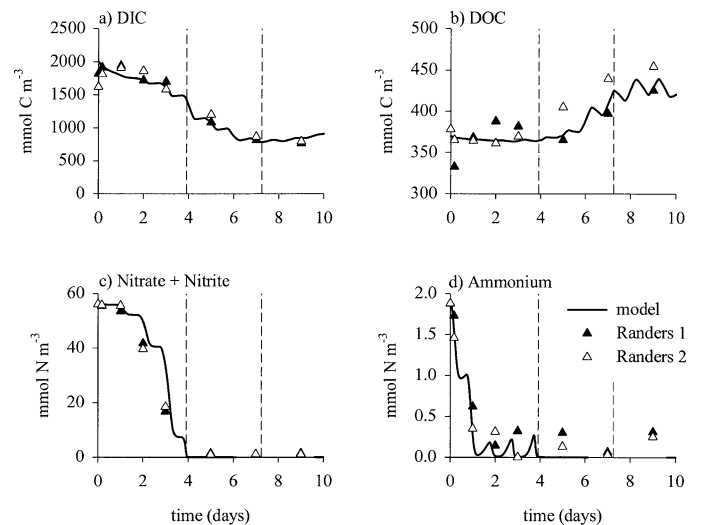


Fig. 3. Temporal evolution of dissolved pools for the two enclosure experiments (Randers 1 and 2) and model results (solid line). The three phases are denoted by vertical dashed lines.

Table 3. Model equations.

(1)	$f(T) = \exp\left[\ln(Q10)\frac{T - 20}{10}\right]$
Phytoplankton	
(2)	$\frac{dP_N}{dt} = (1 - \gamma_1)uptN_p - G_p - M_p$
(3)	$\frac{dP_C}{dt} = (1 - \gamma_1)uptC_p - G_p\theta_p - M_p\theta_p - R_p$
(4)	$uptN_p = uptA_p + uptN_{n,p} = [Q_{N_n}(N_n, A)\mu_{p,N_n} + Q_A(A)\mu_{p,A}]\left(1 - \frac{\min \theta_p}{\theta_p}\right)P_C f(T)$
(5)	$Q_{N_n}(N_n, A) = \frac{N_n \exp(-\psi A)}{k_{N_n} + N_n}$
(6)	$Q_A(A) = \frac{A}{k_A + A}$
(7)	$uptC_p = FQ_C(DIC)\left(1 - \frac{\theta_p}{\max \theta_p}\right)\mu_p P_C f(T)$
(8)	$F = [1 - \exp(-\alpha I/\mu_p)]$
(9)	$Q_C(DIC) = \frac{DIC}{k_{SDIC} + DIC}$
(10)	$E = \gamma_3 FQ_C(DIC)\left(\frac{\theta_p - \min \theta_p}{\max \theta_p}\right)\mu_p P_C f(T)$
(11)	$R_{p,B} = r_{p,B}P_N f(T)$
(12)	$R_{p,A} = r_{p,A}uptC_p$
(13)	$R_p = R_{p,B} + R_{p,A}$
(14)	$M_p = m_p P_N f(T)$
(15)	$M_p\theta_p = m_p P_C f(T)$
Zooplankton	
(16)	$\frac{dZ_N}{dt} = AssN_Z - M_Z - E_Z$
(17)	$AssN_Z = (1 - \varphi)\beta(G_p + G_B + G_D)$
(18)	$AssC_Z = (1 - \varphi)\beta(G_p\theta_p + G_B\theta_B + G_D\theta_D)$
(19)	$G_p = \frac{gZp_1P_N^2}{k_g(p_1P_N + p_2B_N + p_3D_N) + p_1P_N^2 + p_2B_N^2 + p_3D_N^2}f(T)$
(20)	$R_{z,A} = AssC_Z \times f_{z,A}$
(21)	$R_{z,B} = N_Z \times f_{z,B}f(T)$
(22)	$R_Z = R_{z,A} + R_{z,B}$
(23)	$E_Z = AssN_Z - (AssC_Z - R_Z)/\theta_Z$
(24)	$E_Z \leq 0 \Rightarrow R_Z = AssC_Z - AssN_Z \times \theta_Z \quad E_Z = 0$
(25)	$M_Z = \frac{m_z Z_N^2}{K_{\mu_z} + Z_N}f(T)$

Table 3. Continued.

Bacteria

$$(26) \quad \frac{dB_N}{dt} = F_B - G_B - M_B$$

$$(27) \quad \text{upt}C_B = \frac{\mu_B \theta_B B_N L_C}{k_L + L_C}$$

$$(28) \quad \text{upt}N_B = \text{upt}C_B \frac{L_N}{L_C}$$

$$(29) \quad \text{upt}A_B^* = \frac{\mu_B B_N A}{k_A + A}$$

if $-E_B \leq \text{upt}A_B^*$:

$$(30) \quad F_B = \text{upt}C_B \omega / \theta_B$$

$$(31) \quad R_B = \text{upt}C_B (1 - \omega)$$

$$(32) \quad E_B = \text{upt}N_B - U_C \omega / \theta_B$$

if $\text{upt}N_B + \text{upt}A_B^* \leq \text{upt}C_B \times \omega / \theta_B$:

$$(33) \quad F_B = \text{upt}N_B + \text{upt}A_B$$

$$(34) \quad R_B = F_B \theta_B (1 / \omega - \omega)$$

$$(35) \quad E_B = -\text{upt}A_B$$

$$(36) \quad M_B = m_B B_N^3 f(T)$$

Detritus

$$(37) \quad \frac{dD_N}{dt} = (1 - \varphi)(1 - \beta)(G_P + G_B + G_D) + (1 - \varepsilon)M_P - G_D - \text{Dissolution}N$$

$$(38) \quad \text{Dissolution}C = R_{C,\max}(1 - \theta_D / \theta_{D,\max})D_C f(T)$$

$$(39) \quad \text{Dissolution}N = R_{N,\max}(1 - \theta_D / \theta_{D,\max})D_N f(T) \quad \text{if } \theta_D \geq \theta_{D,\max}$$

$$(40) \quad R_{C,\max} < R_{N,\max}$$

$$(41) \quad \left. \begin{array}{l} \text{Dissolution}C = 0 \\ \text{Dissolution}N = 0 \end{array} \right\} \quad \text{if } \theta_D < \theta_{D,\max}$$

DOM

$$(43) \quad \frac{dL_C}{dt} = \gamma_1(E + \text{upt}C_P) + \delta[(1 - \gamma_1)E + \varphi(G_P \theta_P + G_B \theta_B + G_D \theta_D) + \varepsilon m_P P_C + M_B \theta_B + \text{Dissolution}C] + \text{BacterialDOHydrolysis} - \text{upt}C_B$$

$$(44) \quad \frac{dS_C}{dt} = (1 - \delta)[(1 - \gamma_1)E + \varphi(G_P \theta_P + G_B \theta_B + G_D \theta_D) + \varepsilon m_P P_C + M_B \theta_B + \text{Dissolution}C] - \text{BacterialDOHydrolysis}$$

$$(45) \quad \frac{dL_N}{dt} = \gamma_1 \text{upt}N_P + \delta[\varphi(G_P + G_B + G_D) + \varepsilon m_P P_N + M_B + \text{Dissolution}N] + \text{BacterialDONhydrolysis} - \text{upt}N_B$$

$$(46) \quad \frac{dS_N}{dt} = (1 - \delta)[\varphi(G_P + G_B + G_D) + \varepsilon m_P P_N + M_B + \text{Dissolution}N] - \text{BacterialDONhydrolysis}$$

$$(47) \quad \text{BacterialDOHydrolysis} = \mu_S \times B_N \times \frac{S_C}{k_S + S_C} f(T)$$

$$(48) \quad \text{BacterialDONhydrolysis} = \mu_S \times B_N \times \frac{S_N}{k_S + S_C} f(T)$$

Table 3. Continued.

DIN	
(49)	$\frac{dA}{dt} = E_B + E_Z - \nu Af(T) - uptA_p$
(50)	$\frac{dN_n}{dt} = \nu Af(T) - uptN_{n,p}$
DIC	
(51)	$\frac{dDIC}{dt} = R_p + R_z + R_b - uptC_p - E - CO_2 flux$
(52)	$CO_2 flux = K \times [pCO_{2(water)} - pCO_{2(atm)}] \quad pCO_{2(water)} = CO_2/K_0$
	$CO_2 = DIC - [CO_3^{2-}] - [HCO_3^{-}] = DIC \times \frac{H^+ \times H^+}{H^+ \times H^+ + K_{C1} \times H^+ + K_{C1} \times K_{C2}}$
	$H^+ = 10^{-pH}$
Chl <i>a</i>	
(53)	$\eta_p = \min \eta_p + (\max \eta_p - \min \eta_p) \times \frac{\min \theta_p}{\theta_p} \times \frac{\max \theta_p - \theta_p}{\max \theta_p - \min \theta_p}$
(54)	$Chl a = \eta_p \times N_p$

$m^{-3} d^{-1}$) were consistent with those found during 24-h in situ incubations (19.8 and 7.3 $mmol m^{-3} d^{-1}$, respectively; Gattuso pers. comm.). The total nitrogen uptake predicted by the model (5.2 $mmol m^{-3} d^{-1}$) was somewhat higher than the sum of ammonium, nitrate, urea, and dissolved free amino acids uptake measured during 2-h incubations (4.8 $mmol m^{-3} d^{-1}$; Veuger pers. comm.).

Fluxes between the compartments, averaged over the three phases (bloom, intermediate, and stationary), were calculated and are shown in Fig. 6. The magnitude and fate of phytoplankton production is shown in Table 4, and the charac-

teristics of the microbial loop are shown in Table 5. In the phytoplankton bloom phase (Fig. 6a), phytoplankton production was only light-limited, and most of the carbon and nitrogen assimilated resulted in algal biomass accumulation (84% and 93% for C and N, respectively). Only a small fraction (2%) of the assimilated carbon and nitrogen was released to the dissolved organic pool or was lost by predation and senescence mortality (3.4% and 3.9% for C and N, respectively; Table 4). Heterotrophic mechanisms contributed the most to the formation of DOM (56% and 63% in terms of C and N, respectively), which was produced with an average C:N ratio of ~ 7 . The uptake of DOM by bacteria was used for growth (19% and 30% for C and N, respec-

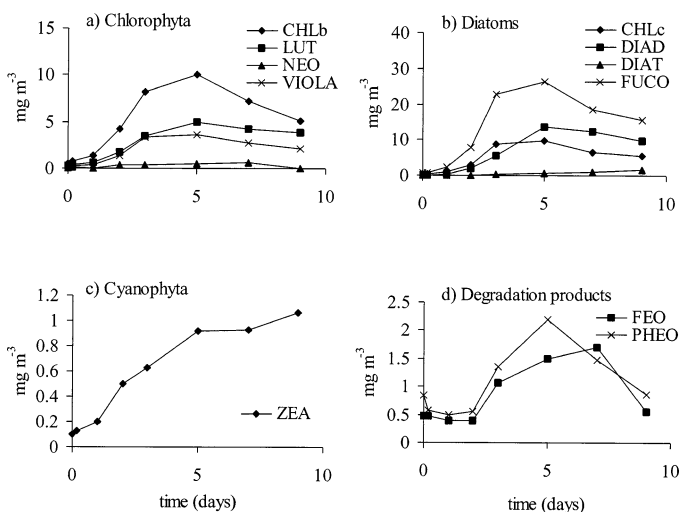


Fig. 4. Temporal evolution of photosynthetic pigments characteristic for (a) green algae, (b) diatoms, (c) cyanobacteria, and (d) degradation products. CHLb: Chl *b*, CHLc: Chl *c*, DIAD: diadinoxanthine, DIAT: diatoxanthine, FEO: pheophytine, FUCO: fucoxanthine, LUT: luteine, NEO: neoxanthine, PHEO: pheophorbide, VIOLA: violaxanthine, ZEA: zeaxanthine.

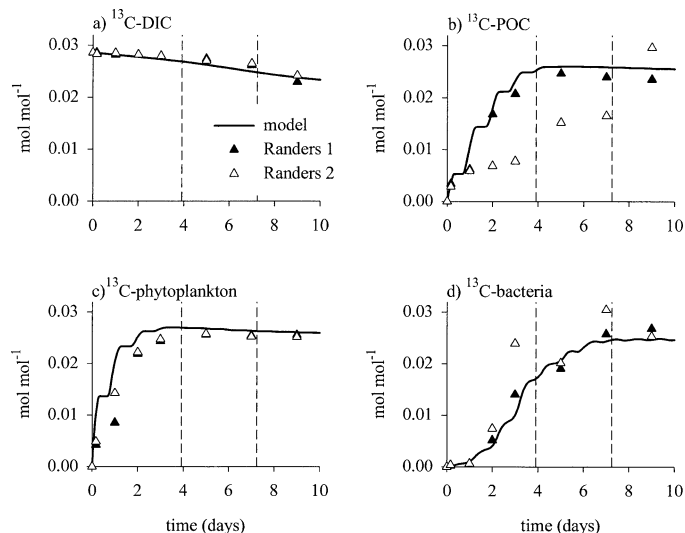
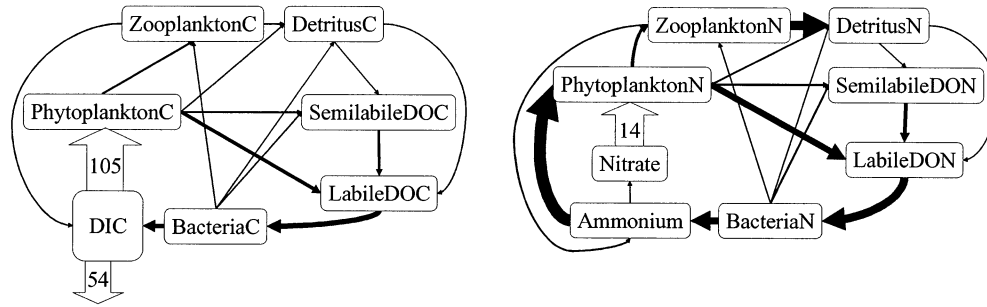
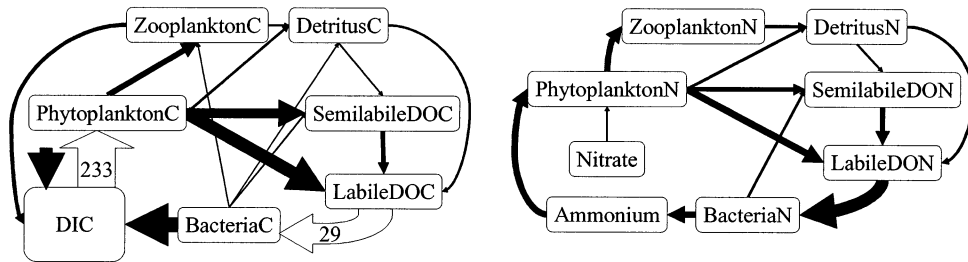


Fig. 5. Temporal evolution of ^{13}C fractions in DIC, POC, and algal and bacterial carbon pools for the two enclosure experiments (Randers 1 and 2) and model results (solid line).

a) Bloom phase



b) Intermediate phase



c) Nutrient depleted phase

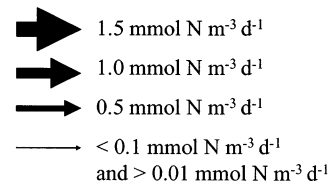
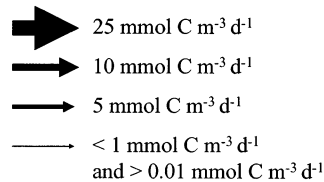
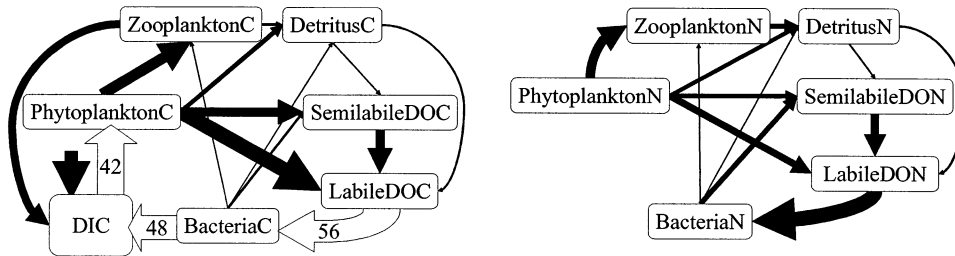


Fig. 6. Carbon (left) and nitrogen (right) flows during the three phases; the arrow thickness of the black arrows is proportional to the flux rate. Fluxes $>25 \text{ mmol C m}^{-3} \text{ d}^{-1}$ and $1.5 \text{ mmol N m}^{-3} \text{ d}^{-1}$, respectively, are represented with open arrows, with the flux indicated in $\text{mmol m}^{-3} \text{ d}^{-1}$. Fluxes $<0.01 \text{ mmol m}^{-3} \text{ d}^{-1}$ are not shown. (a) Bloom phase (days 1–3); (b) intermediate, unbalanced growth phase (days 4–7); (c) final, nutrient-depleted phase (days 8–9).

tively), respiration (81% of C), and ammonium regeneration (70% of N; Table 5). During this phase, there was an efflux of CO_2 because of initial high $p\text{CO}_2$ values.

In the intermediate, unbalanced growth phase (Fig. 6b), the carbon cycle had a pattern similar to the bloom phase, whereas the nitrogen cycle showed the characteristics of a nutrient-limited ecosystem. Gross primary production was about twice that during the bloom phase, but biomass-specific gross primary production was only 33% of that during the previous period. Approximately 71% of this assimilated carbon added to phytoplankton biomass, 11% was released as DOC (mainly by exudation), and $\sim 7\%$ was lost by zoo-

plankton grazing and mortality. In contrast, the algal nitrogen uptake dropped to very low values and was not sufficient to overcome losses by mortality, such that the algal nitrogen content decreased during this phase. DOC production came from algal exudation (60%) and heterotrophic mechanisms (40%), whereas almost all DON was produced by heterotrophic processes ($>99\%$). Algal exudation was high, to overcome excess carbon assimilation, and this resulted in an overall DOC: DON production ratio of >29 . The DON consumed by bacteria was mainly used for growth (73%), and the remaining 27% was excreted as ammonium.

During the final, stationary phase (Fig. 6c), both carbon

Table 4. Magnitude and fate of the phytoplankton primary production (PP) and N uptake. Rates are in $\text{mmol C m}^{-3} \text{d}^{-1}$ and $\text{mmol N m}^{-3} \text{d}^{-1}$, and concentrations are in mmol m^{-3} . Numbers in bold are concentrations.

Phytoplankton	Bloom	Intermediate	Nutrient limited
C	114.3	786.7	881.8
Gross PP	118.3	263.7	51.3
>Growth	98.8	186.5	-21.4
>Respiration	13.0	30.4	9.4
>Mortality	4.0	17.7	29.9
>DOC exudation	2.0	28.7	33.3
N	17.8	52.5	45.0
N uptake	15.3	0.6	0.0
>Growth	14.3	-1.0	-2.1
>Mortality	0.6	1.6	2.1
>DON exudation	0.3	0.01	0.0

and nitrogen acquisition of the phytoplankton were limited. Photosynthesis and carbon fixation were limited by the algal physiological condition (as represented by the high internal C:N ratio), whereas nitrogen uptake was zero because there was no dissolved inorganic nitrogen. Neither C nor N assimilation was sufficient to maintain a positive balance, and 65% of photosynthetic carbon products were exudated. Mortality (caused by zooplankton grazing or senescence) was responsible for the decline of the algal concentration and kept increasing, despite the decline in phytoplankton biomass (Fig. 2e,f). Both carbon and nitrogen cycling were dominated by the microbial loop during this phase. Similar to the intermediate phase, DOC was derived from algal exudation (56%) and heterotrophic mechanisms (44%), whereas all DON production came from heterotrophic mechanisms, such as mortality, grazing, and detritus breakdown. The overall DOC:DON production ratio was 27 because of the exudation of carbon-rich DOM by algae. During this postbloom phase, all DON consumed served growth of the bacteria, and there was no ammonium excretion.

Discussion

Algae and bacteria are exposed to continuously varying environmental conditions. These fluctuations have major consequences for their interaction and for their carbon and nitrogen cycles. We induced changes in the environment by enclosing riverine, nutrient-rich waters under batch conditions. Most of our experimental results were consistent with and confirmed results of previous studies of marine systems. However, by administering a deliberate tracer (^{13}C) and the use of a state-of-the-art ecosystem model, not only did we obtain a more complete and consistent picture of ecosystem functioning and carbon and nitrogen cycling, but we were also able to quantify the links between algae and bacteria and between carbon and nitrogen dynamics and to sharpen the modeling tools that represent these processes.

Experimental blooms in enclosures and mesocosms have shown exponential growth of algae with tight covariation of carbon and nutrients, increases in pH, and little DOC accumulation as long as nutrients were replete (Antia et al. 1963; Banse 1994; Alldredge et al. 1995; Sondergaard et al. 2000; Engel et al. 2002). Maximum Chl *a* concentrations were usually observed near the time of nutrient depletion (Alldredge et al. 1995; Norrman et al. 1995; Engel et al. 2002). After nutrient depletion, carbon and nitrogen dynamics were usually decoupled, as reflected in the accumulation of DOC (Banse 1994; Norrman et al. 1995; Sondergaard et al. 2000), increases in particulate C:N ratios caused by excess particulate carbon (Banse 1994; Alldredge et al. 1995; Engel et al. 2002), and release of carbon-rich DOM (Biddanda and Benner 1997; Wetz and Wheeler 2003). Most of these studies involved the addition of nutrients and focused on the uncoupling of POC and PN dynamics (Alldredge et al. 1995; Engel et al. 2002). The results of our enclosure experiment with natural river water confirm these literature observations for experimental marine systems and are also consistent with field observations regarding the uncoupling of carbon and nitrogen dynamics (Sambrotto et al. 1993), the accumulation of carbon-rich DOM after the spring bloom (Duursma 1961), and the delayed response of bacteria to increased primary production (Ducklow et al. 1993; Ducklow 1999).

Table 5. Characteristics of the bacterial loop. Rates are in $\text{mmol C m}^{-3} \text{d}^{-1}$ and $\text{mmol N m}^{-3} \text{d}^{-1}$, and concentrations are in mmol m^{-3} . Numbers in bold are concentrations.

	Bloom	Intermediate	Nutrient limited
Bacterial C	8.9	15.1	26.5
DOC production	5.8	48.0	59.9
By exudation	2.5	28.7	33.3
By heterotrophic mechanisms	3.3	19.3	26.6
DOC uptake	7.2	30.2	59.7
Bacterial growth	1.4	5.7	11.3
Bacterial N	1.8	3.0	5.2
DON production	0.8	1.6	2.3
By exudation	0.3	0.01	0.0
By heterotrophic mechanisms	0.5	1.6	2.3
DON uptake	0.9	1.5	2.2
Bacterial growth	0.3	1.1	2.2

Norrman et al. (1995) studied the production and consumption of DOC during an experimental diatom bloom using ^{13}C -bicarbonate as a deliberate tracer; bacteria were traced using nucleic acids as a biomarker. They observed rapid labeling and isotopic equilibration of the POC pool after 7 d and a delayed appearance of ^{13}C in the DOC and bacterial pools. The DOC and bacterial pools did not reach isotopic equilibrium during the 14-d period of the experiment. Our experimental results confirm but also complement these results. In our experiment, the added ^{13}C -bicarbonate was rapidly fixed by phytoplankton, which resulted in isotope equilibration of phytoplankton carbon by day 3 (Fig. 5c). The POC pool, which was composed of algae, bacteria, and detritus, was consequently also rapidly labeled, but equilibration took 1 d more (Fig. 5b). Although full isotopic equilibration of the bacterial carbon pool was reached by day 6 (Fig. 5d), there was a delay of at least 1 d before significant amounts of ^{13}C appeared in specific bacterial PLFA. Norrman et al. (1995) did not observe this delay, likely because they only measured the bacterial ^{13}C content after 3.5 d. In addition, bacteria did not attain full isotope equilibration in their experiments, which they attributed to a potential artefact caused by the nucleic acid method, the presence of a population of inactive bacteria, and the use of old and new DOC by the bacteria. The biomarkers we used specifically trace active bacteria, which could explain the difference in extent of isotopic equilibration, although differences in the ecosystem functioning (the roles of background DOC and grazing on bacteria) cannot be ruled out.

Carbon and nitrogen coupling by phytoplankton—In general, the ecosystem in our enclosures reacted faster than those in other enclosure studies (Alldredge et al. 1995; Norrman et al. 1995; Engel et al. 2002). As a consequence, it was possible to clearly delineate three phases with distinct carbon-nitrogen relationships rather than the nutrient-replete and -depleted phase reported in earlier studies. During the exponential growth phase (days 0–3) the algae were light-limited and took up carbon and nitrogen in constant ratios (~ 6) until the exhaustion of nutrients. The C:N ratio of the particulate pool decreased from 10 to 7 (Fig. 7). During the intermediate, unbalanced growth phase (days 4–7), algal carbon assimilation continued at a high rate, whereas nitrogen assimilation was strongly nutrient limited and the C:N ratio of algae rapidly increased until it reached its maximum level (~ 20). This is reflected in the increase of the C:N ratio of the particulate pool from 7 to 16 (Fig. 2). Finally, during the stationary phase, both algal carbon and nitrogen assimilation were limited, the former by algal physiology and the latter by the external nutrient concentrations, and the C:N ratio of algal and particulate organic matter pools remained high (days 8–9).

The initial decrease of particulate organic matter C:N ratios and the subsequent increase after dissolved inorganic nitrogen depletion has been reported before (Banse 1994; Alldredge et al. 1995) and was attributed to preferential PON degradation, the formation of transparent extracellular particles (TEP), and an intracellular increase in algal C:N ratios (Engel et al. 2002). Our model did not include the formation of TEP but accounted for both preferential PN dissolution

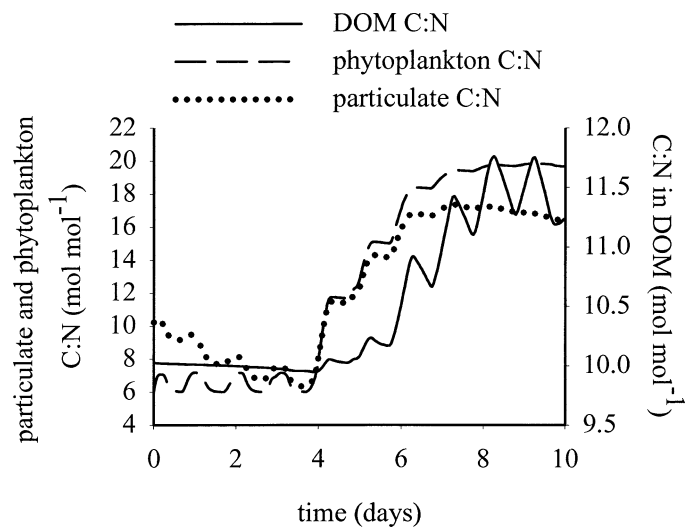


Fig. 7. Modeled temporal evolution of C:N ratios of the DOM, particulate organic, and phytoplankton pools.

and the unbalanced acquisition of carbon and nitrogen in phytoplankton (Fig. 7). The initial decrease of C:N ratios (days 0–3) was merely caused by the dilution of the detrital pool (C:N = 20) with newly formed phytoplankton (C:N ~ 6), whereas the increase in the C:N ratio after nutrient depletion was consistent with intracellular increases of algal C:N ratios, as represented in the unbalanced growth model of Tett (1998).

The unbalanced uptake of carbon and nitrogen allows algae to continue photosynthesis under temporarily nutrient-limited conditions. It is the main cause of the uncoupling of carbon and nitrogen flows in the ecosystem and is expressed by a more than doubling of the particulate C:N ratio in 2 d (Fig. 7). However, prolonged nutrient limitation results in the exudation of excess carbon as DOM. The exudation of carbon-rich DOM by algae is another mechanism by which the flows of carbon and nitrogen are decoupled. It causes increases in DOC:DON ratios of $>10\%$ in 2 d, lagging ~ 1 d behind the rise in the particulate C:N ratio (Fig. 7).

The production of DOM—Major research efforts during the past decade have revealed a number of the mechanisms that result in the formation of DOM (Carlson 2002). The relative importance of these different DOM sources is unknown and likely depends on ecosystem functioning. It is instructive to distinguish between the release of DOM by autotrophic and heterotrophic mechanisms, because the governing factors differ. The heterotrophic release of DOM is caused by the dissolution of particulate detritus (Smith et al. 1992), zooplankton sloppy feeding, and the incomplete ingestion (Jumars et al. 1989) and lysis of bacteria (Anderson and Williams 1998). Phytoplankton release may either occur passively (leakage and algal lysis, Bjørnsen 1988) or may consist of active exudation of carbon-rich DOM (Biddanda and Benner 1997; Carlson 2002). These two autotrophic DOM sources differ in their C:N ratio and governing factors. Although passive leakage is proportional to biomass or production (as we assumed in our model), active exudation

depends strongly on algal physiological status, in particular light and nutrient availability (Obernosterer and Herndl 1995; Anderson and Williams 1998; Carlson 2002).

The quantitative importance of these processes under in situ conditions is still unclear, and our results clearly indicate that they may vary rapidly during and after bloom events. During the nutrient-rich bloom period, there was no active DOC exudation by phytoplankton, and ~2% of the fixed C and N was released as DOM with a C:N ratio similar to that assimilated. Heterotrophic mechanisms accounted for 60% of total DOM production during that period, and the DOM produced had a C:N ratio of 7. During the intermediate and stationary phases, algal exudation of recently fixed carbon increased and became the most important DOC source; during the stationary phase, 65% of the carbon assimilated was exudated. Heterotrophic sources of DOM also increased as a consequence of higher concentration of phytoplankton, detritus, and bacteria and were relatively N rich: heterotrophic and autotrophic DOM C:N production ratios were ~11.7 versus 28, respectively. Overall, the main source of DOC was phytoplankton exudation (almost 60% of the DOC production) and not detritus decay. Heterotrophic processes were the main source of DON (94%).

Percentages of extracellular release (PER) of recently fixed carbon vary widely from not significant up to 70% of total production (Norrman et al. 1995; Anderson and Williams 1998; Carlson 2002). This variability has been related to many factors, including nutrient availability, phytoplankton size, and net community production (Teira et al. 2001). It is unclear whether the increase in DOC release under nutrient-stressed conditions is caused by the preponderance of small cells with higher surface: volume ratios and, therefore, a higher capacity of passive leakage of DOC (Bjørnsen 1988), to the physiological condition of the algae (Dubinsky and Berman-Frank 2001), or a combination of both. By implementing the stress-dependent formulation for DOC exudation as described in A&W, we chose the latter explanation, first because of the large changes in the particulate C:N ratio, which demonstrated unbalanced growth of phytoplankton and thus changing physiological conditions that preceded the increases in DOC concentrations; and, second, there was no indication that a shift toward smaller cells occurred in the experiments—on the contrary, an inspection of the pigment concentrations reflected a relative increase in diatoms, which are generally larger than flagellates and green algae. Teira et al. (2001) reported high PER values in the oligotrophic Atlantic Ocean, with net negative community production and low PER values for upwelling conditions with net community productions. The results of our enclosure study support these field observations and also show that the transition between different levels of phytoplankton DOC exudation can be rapid.

Algal-bacterial interactions—Heterotrophic bacteria are the major sink for marine DOM, which provides the carbon and the majority of the nitrogen for the bacteria. Most of the DOM originates directly (via exudation) or indirectly (via food-web interactions) from phytoplankton, and, as such, bacteria depend on algae for growth. The pool of DOM does not always provide enough nitrogen to sustain bacterial

growth, in which case they will assimilate dissolved inorganic nitrogen (Wheeler and Kirchman 1986; Kirchman 1994; Middelburg and Nieuwenhuize 2000; Joint et al. 2002) rather than excrete it. Unfavorable DOC:DON ratios for bacterial growth result in particular from algal exudation of carbon-rich DOM, a process that is stimulated under nutrient-stressed conditions. Thus, paradoxically, nutrient stress induces the algae to produce carbon substrates suitable for growth of bacteria, which then compete with the algae for nutrients (Bratbak and Thingstad 1985).

Algal-bacterial interactions in our experimental bloom study changed from commensalism at the start to nutrient competition during the final phase. The three phases comprise almost the entire spectrum of trophic pathways (Legendre and Rassoulzadegan 1995). During the first phase (the herbivory/multivorous food web; sensu Legendre and Rassoulzadegan 1995), bacteria consumed DOM from autotrophic and heterotrophic sources and were regenerating ammonium, available for algal growth. The ^{13}C data indicated that there was a delay in the transfer of recently fixed carbon to the bacterial pool (Fig. 5). Such a delay between carbon fixation and bacterial response is consistent with many field observations that have shown a time lag between phytoplankton blooms and bacterial increase (Ducklow 1999); it is caused by the mixed DOM sources during the initial phase (passive leakage and heterotrophic sources) and the presence of allochthonous DOM. Algal-bacterial interactions during the intermediate phase resembled a microbial food web sensu Legendre and Rassoulzadegan (1995), with limited nitrogen uptake by the algae caused by low dissolved inorganic nitrogen concentrations and limited ammonium regeneration by the bacteria. Bacteria were mainly depending on algal exudates, and there was a direct transfer of ^{13}C from algae to bacteria such that the bacterial pool became fully labeled by day 6. During the stationary phase, there was no regeneration of ammonia by bacteria, and both algal and bacterial growth was nitrogen limited. This last stage resembled a typical microbial loop-dominated ecosystem. There was some DOC accumulation during this stage, which was due to the “malfunctioning of the microbial loop” caused by nutrient limitation of bacterial growth (Thingstad and Havskum 1999), such that DOC uptake cannot keep pace with its exudation by phytoplankton.

The three phases have distinct ratios between bacterial and algal parameters. Bacterial to primary production (BP:PP) ratios increased from 0.01 via 0.02 to 0.22 during the experiment. Similarly, bacterial carbon demand to primary production (BCD:PP) ratios increased from 0.06 at the beginning over 0.12 during the intermediate stage to 1.16 at the end. These ratios are often used to assess the metabolic status and functioning of ecosystems and to quantify the coupling of phytoplankton and heterotrophic bacteria (Anderson and Ducklow 2001; Morán et al. 2002). High BCD:PP ratios indicate that bacteria dominate carbon flows, and values >1 imply an excess of carbon consumption by bacteria over algal production. This is often used as a measurement of net heterotrophy, but care should be taken, because BP and thus BCD are not constrained by PP (Strayer 1988; Jahnke and Craven 1995) and because changes in organic carbon stocks

may support imbalances in production and consumption processes for some time (Figs. 2, 3).

Combined modeling and stable isotope approach—The coupled experimental modeling approach we used provides unique opportunities to test and fine-tune our current state of knowledge of ecosystem functioning and, more specifically, of carbon and nitrogen coupling. Moreover, by the model, we were able to analyze all the flows, even though only few of them have been measured. Models, as simple and crude as they may appear, capture our understanding of a system in mathematical terms, and the consequences of this understanding, model output, are easily compared with observations. Our enclosure experiments were especially designed to allow model-data comparison. To describe the experiments, we chose a model complexity that was paralleled by the available data. This included combining a simple description of algal unbalanced growth that describes algae in terms of C and N (Tett 1998) with a more complex bacterial growth model (Anderson and Williams 1998), including two distinct DOC and DON pools with different biological lability. Although the experimental bloom evolved within a few days from a carbon and nitrogen balanced herbivorous/multivorous ecosystem to microbial loop system (Legendre and Rassoulzadegan 1995), our simple model reproduced these changes in ecosystem functioning quite well and therefore provides an avenue toward generic ecosystem models.

The ^{13}C measurements, and especially the resolution of algal and bacterial compartments using specific PLFA biomarkers (Boschker and Middelburg 2002), proved to be crucial to determine the phytoplankton exudation rates and the bacterial turnover rates. We had to find a delicate balance between reconciling the observed delay in bacterial ^{13}C uptake and reproducing the increased concentration of bacteria during the postbloom phase. Sensitivity analysis of the parameters (not shown) demonstrated that the initial slow bacterial uptake of ^{13}C was significantly influenced by the phytoplankton leakage rate. Moreover, the additional DOC exudation by phytoplankton under nutrient-limiting conditions influenced the bacterial ^{13}C content. Without the ^{13}C labeling, it would not have been possible to determine the DOC production and uptake rates; in that case, it would not have been possible to distinguish exudated DOC from recycled DOC that comes from bacteria or detritus.

References

- ALLDREDGE, A. L., C. C. GOTSCHALK, U. PASSOW, AND U. RIEBESELL. 1995. Mass aggregation of diatom blooms: Insights from a mesocosm study. *Deep-Sea Res. II* **42**: 9–27.
- ANDERSON, T. R., AND H. W. DUCKLOW. 2001. Microbial loop carbon cycling in ocean environments studied using a simple steady-state model. *Aquat. Microb. Ecol.* **26**: 37–49.
- , AND P. J. L. WILLIAMS. 1998. Modelling the seasonal cycle of dissolved organic carbon at station E1 in the English Channel. *Estuar. Coast. Shelf Sci.* **46**: 93–109.
- ANTIA, N. J., C. D. McALLISTER, T. R. PARSONS, K. STEPHENS, AND J. D. H. STRICKLAND. 1963. Further measurements of primary production using a large-volume plastic sphere. *Limnol. Oceanogr.* **8**: 166–183.
- BANSE, K. 1994. Uptake of inorganic carbon and nitrate by marine plankton and the Redfield ratio. *Global Biogeochem. Cycles* **8**: 81–84.
- BARRANGUET, C., P. M. J. HERMAN, AND J. J. SINKE. 1997. Microphytobenthos biomass and community composition studied by pigment biomarkers: Importance and fate in the carbon cycle of a tidal flat. *J. Sea Res.* **38**: 59–70.
- BIDDANDA, B., AND R. BENNER. 1997. Carbon, nitrogen, and carbohydrate fluxes during the production of particulate dissolved organic matter by marine phytoplankton. *Limnol. Oceanogr.* **42**: 506–518.
- BJØRNSSEN, P. K. 1988. Phytoplankton exudation of organic matter: Why do healthy cells do it? *Limnol. Oceanogr.* **33**: 151–154.
- BOSCHKER, H. T. S., J. F. C. DE BROUWER, AND T. E. CAPPENBERG. 1999. The contribution of macrophyte-derived organic matter to microbial biomass in salt-marsh sediments: Stable carbon isotope analysis of microbial biomarkers. *Limnol. Oceanogr.* **44**: 309–319.
- , AND J. J. MIDDELBURG. 2002. Stable isotopes and biomarkers in microbial ecology. *FEMS Microbiol. Ecol.* **40**: 85–95.
- BRATBAK, G., AND T. F. THINGSTAD. 1985. Phytoplankton-bacteria interactions: An apparent paradox? Analysis of a model system with both competition and commensalisms. *Mar. Ecol. Prog. Ser.* **25**: 23–30.
- BRINCH-IVERSEN, J., AND G. M. KING. 1990. Effects of substrate concentration, growth state, and oxygen availability on relationships among bacterial carbon, nitrogen and phospholipid phosphorus content. *FEMS Microbiol. Ecol.* **74**: 345–356.
- CARLSON, C. A. 2002. DOM lability, p. 123–133. *In* D. A. Hansell and C. A. Carlson [eds.], *Biogeochemistry of marine dissolved organic matter*. Academic.
- CHRISTIAN, J. R., AND T. R. ANDERSON. 2002. Modelling DOM biogeochemistry, p. 717–755. *In* D. A. Hansell and C. A. Carlson [eds.], *Biogeochemistry of marine dissolved organic matter*. Academic.
- COLE, J. J., S. R. CARPENTER, J. F. KITCHELL, AND M. L. PACE. 2002. Pathways of organic carbon utilization in small lakes: Results from a whole-lake ^{13}C addition and coupled model. *Limnol. Oceanogr.* **47**: 1664–1675.
- COTNER, J. B., AND B. A. BIDDANDA. 2002. Small players, large role: Microbial influence on biogeochemical processes in pelagic aquatic ecosystems. *Ecosystems* **5**: 105–121.
- DEL GIORGIO, P. A., AND J. J. COLE. 1998. Bacterial growth efficiency in natural aquatic systems. *Annu. Rev. Ecol. Syst.* **29**: 503–541.
- DROOP, M. R. 1973. Some thoughts on nutrient limitation in algae. *J. Phycol.* **9**: 264–272.
- DUBINSKY, Z., AND I. T. BERMAN-FRANK. 2001. Uncoupling primary production from population growth in photosynthesizing organisms in aquatic ecosystems. *Aquat. Sci.* **63**: 4–17.
- DUCKLOW, H. W. 1999. The bacterial component of the oceanic euphotic zone. *FEMS Microbiol. Ecol.* **30**: 1–10.
- , D. L. KIRCHMANN, H. L. QUINBY, C. A. CARLSON, AND H. G. DAM. 1993. Stocks and dynamics of bacterioplankton carbon during the spring bloom in the Eastern Atlantic Ocean. *Deep-Sea Res. II* **40**: 245–263.
- DUURSMA, E. K. 1961. Dissolved organic carbon, nitrogen and phosphorus in the sea. *Neth. J. Sea. Res.* **1**: 1–147.
- ENGEL, A., S. GOLDTHWAIT, U. PASSOW, AND A. ALLDREDGE. 2002. Temporal decoupling of carbon and nitrogen dynamics in a mesocosm diatom bloom. *Limnol. Oceanogr.* **47**: 753–761.
- FLYNN, K. J., AND M. J. R. FASHAM. 2003. Operation of light-dark cycles within simple ecosystem models of primary production and the consequences of using phytoplankton models with different abilities to assimilate N in darkness. *J. Plankton Res.* **25**: 83–92.

- GEIDER, R. J., H. L. MACINTYRE, AND T. M. KANA. 1998. A dynamic regulatory model of phytoplankton acclimation to light, nutrients, and temperature. *Limnol. Oceanogr.* **43**: 679–694.
- JAHNKE, R. A., AND D. B. CRAVEN. 1995. Quantifying the role of heterotrophic bacteria in the carbon cycle—a need for respiration rate measurements. *Limnol. Oceanogr.* **40**: 436–441.
- JOINT, I., P. HENRIKSEN, G. A. FONNES, D. BOURNE, T. F. THINGS-TAD, AND B. RIEMANN. 2002. Competition for inorganic nutrients between phytoplankton and bacterioplankton in nutrient manipulated mesocosms. *Aquat. Microb. Ecol.* **29**: 145–159.
- JUMARS, P. A., D. L. PENRY, J. A. BAROSS, M. J. PERRY, AND B. W. FROST. 1989. Closing the microbial loop—dissolved carbon pathway to heterotrophic bacteria from incomplete ingestion, digestion and absorption in animals. *Deep-Sea Res.* **36**: 483–495.
- KIRCHMAN, D. L. 1994. The uptake of inorganic nutrients by heterotrophic bacteria. *Microb. Ecol.* **28**: 255–271.
- LANCELOT, C., AND G. BILLEN. 1985. Carbon-nitrogen relationships in nutrient metabolism of coastal marine ecosystems. *Adv. Aquat. Microbiol.* **3**: 263–321.
- , ———, C. VETH, S. BECQUEVORT, AND S. MATHOT. 1991. Modeling carbon cycling through phytoplankton and microbes in the Scotia-Weddell Sea area during sea ice retreat. *Mar. Chem.* **35**: 305–324.
- LEGENDRE, L., AND F. RASSOULZADEGAN. 1995. Plankton and nutrient dynamics in marine waters. *Ophelia* **41**: 153–172.
- LEVY, M., L. MEMERY, AND J. M. ANDRE. 1998. Simulation of primary production and export fluxes in the Northwestern Mediterranean Sea. *J. Mar. Res.* **56**: 197–238.
- LYCHE, A., T. ANDERSEN, K. CHRISTOFFERSEN, D. O. HESSEN, P. H. B. HANSEN, AND A. KLYSNER. 1996. Mesocosm tracer studies. 2. The fate of primary production and the role of consumers in the pelagic carbon cycle of a mesotrophic lake. *Limnol. Oceanogr.* **41**: 475–487.
- MAGUE, T. H., E. FRIBERG, D. J. HUGHES, AND I. MORRIS. 1980. Extracellular release of carbon by marine phytoplankton: A physiological approach. *Limnol. Oceanogr.* **25**: 262–279.
- MCALLISTER, C. D., N. SHAH, AND J. D. H. STRICKLAND. 1964. Marine phytoplankton photosynthesis as a function of light intensity: A comparison of methods. *J. Fish. Res. Board Can.* **21**: 159–181.
- MIDDELBURG, J. J., C. BARRANQUET, H. T. S. BOSCHKER, P. M. J. HERMAN, T. MOENS, AND C. H. R. HEIP. 2000. The fate of intertidal microphytobenthos carbon: An in situ C-13-labeling study. *Limnol. Oceanogr.* **45**: 1224–1234.
- , AND J. NIEUWENHUIZE. 2000. Nitrogen uptake by heterotrophic bacteria and phytoplankton in the nitrate-rich Thames estuary. *Mar. Ecol. Prog. Ser.* **203**: 13–21.
- MILLERO, F. J. 1995. Thermodynamics of the carbon-dioxide system in the oceans. *Geochim. Cosmochim. Acta* **59**: 661–677.
- MOODLEY, L., AND OTHERS. 2000. Ecological significance of benthic Foraminifera: C-13 labelling experiments. *Mar. Ecol. Prog. Ser.* **202**: 289–295.
- MORÁN, X. A. G., M. ESTRADA, J. M. GASOL, AND C. PEDROS-ALIO. 2002. Dissolved primary production and the strength of phytoplankton bacterioplankton coupling in contrasting marine regions. *Microb. Ecol.* **44**: 217–223.
- NIEUWENHUIZE, J., Y. E. M. MAAS, AND J. J. MIDDELBURG. 1994. Rapid analysis of organic carbon and nitrogen in particulate materials. *Mar. Chem.* **45**: 217–224.
- NORRMAN, B., U. L. ZWEIFEL, C. S. HOPKINSON, AND B. FRY. 1995. Production and utilization of dissolved organic carbon during an experimental Diatom bloom. *Limnol. Oceanogr.* **40**: 898–907.
- OBERNOSTERER, I., AND G. J. HERNDL. 1995. Phytoplankton extracellular release and bacterial growth—dependence on the inorganic N-P ratio. *Mar. Ecol. Prog. Ser.* **116**: 247–257.
- SAMBROTTO, R. N., AND OTHERS. 1993. Elevated consumption of carbon relative to nitrogen in the surface ocean. *Nature* **363**: 248–250.
- SMITH, C. L., AND P. TETT. 2000. A depth-resolving numerical model of physically forced microbiology at the European shelf edge. *J. Mar. Syst.* **26**: 1–36.
- SMITH, D. C., M. SIMON, A. L. ALLDREDGE, AND F. AZAM. 1992. Intense hydrolytic enzyme-activity on marine aggregates and implications for rapid particle dissolution. *Nature* **359**: 139–142.
- SOETAERT, K., V. DECLIPPELE, AND P. HERMAN. 2002. FEMME, a flexible environment for mathematically modelling the environment. *Ecol. Model.* **151**: 177–193.
- , AND OTHERS. 2001. Numerical modelling of the shelf break ecosystem: Reproducing benthic and pelagic measurements. *Deep-Sea Res. II* **48**: 3141–3177.
- SONDERGAARD, M., AND OTHERS. 2000. Net accumulation and flux of dissolved organic carbon and dissolved organic nitrogen in marine plankton communities. *Limnol. Oceanogr.* **45**: 1097–1111.
- STEEMANN NIELSEN, E., AND V. K. HANSEN. 1959. Measurements with the carbon-14 technique of the respiration rates in natural populations of phytoplankton. *Deep-Sea Res. II* **5**: 222–233.
- STERNER, R. W., AND J. J. ELSER. 2003. Ecological stoichiometry: The biology of elements from molecules to the biosphere. Princeton Univ. Press.
- STRAYER, D. 1988. On the limits to secondary production. *Limnol. Oceanogr.* **33**: 1217–1220.
- TEIRA, E., M. J. PAZO, P. SERRET, AND E. FERNANDEZ. 2001. Dissolved organic carbon production by microbial populations in the Atlantic Ocean. *Limnol. Oceanogr.* **46**: 1370–1377.
- TETT, P. 1998. Parameterising a microplankton model. Department of Biological Sciences, Napier Univ.
- THINGSTAD, T. F., AND H. HAVSKUM. 1999. Bacteria-protist interactions and organic matter degradation under P-limited conditions: Analysis of an enclosure experiment using a simple model. *Limnol. Oceanogr.* **44**: 62–79.
- VALLINO, J. J. 2000. Improving marine ecosystem models: Use of data assimilation and mesocosm experiments. *J. Mar. Res.* **58**: 117–164.
- WETZ, M. S., AND P. A. WHEELER. 2003. Production and partitioning of organic matter during simulated phytoplankton blooms. *Limnol. Oceanogr.* **48**: 1808–1817.
- WHEELER, P. A., AND D. L. KIRCHMAN. 1986. Utilization of inorganic and organic nitrogen by Bacteria in marine systems. *Limnol. Oceanogr.* **31**: 998–1009.
- WILLIAMS, P. J. L. 1990. The importance of losses during microbial growth: commentary on the physiology, measurement and ecology of the release of dissolved organic material. *Mar. Microb. Food Webs* **4**: 103–116.

Received: 10 July 2003

Accepted: 9 December 2003

Amended: 31 December 2003